Available online at www.sciencedirect.com
ScienceDirect
Journal of Magnetic Resonance 191 (2008) 267–272
JMR Journal of Magnetic Resonance
www.elsevier.com/locate/jmr

# A rapid measurement of flow propagators in porous rocks

J. Mitchell [a], A.J. Sederman [a], E.J. Fordham [b], M.L. Johns [a], L.F. Gladden [a,*]

[a] Department of Chemical Engineering, University of Cambridge, Pembroke Street, Cambridge CB2 3RA, United Kingdom
[b] Schlumberger Cambridge Research Ltd., High Cross, Madingley Road, Cambridge CB3 0HG, United Kingdom

Received 8 October 2007; revised 12 December 2007
Available online 31 December 2007

**Abstract**

NMR flow propagators have been obtained for brine flowing through Bentheimer sandstone using the rapid DiffTrain pulse sequence. In this way, 8 flow propagators at different observation times Δ were acquired in 67 mins, compared to 7 h for the same measurements implemented with conventional pulsed field gradient (PFG) sequences. DiffTrain allows this time saving to be achieved through the acquisition of multiple displacement probability distributions over a range of Δ in a single measurement. If only the propagator moments are required, this experiment time can be further reduced to 9 mins through appropriate sparse sampling at low $q$ values. The propagator moments obtained from DiffTrain measurements with dense and sparse $q$-space sampling are shown to be equivalent to those obtained from conventional PFG measurements.


*Keywords:* DiffTrain; Flow propagators; Propagator moments; Permeable rocks; $q$-Space sampling

## 1. Introduction

The accurate measurement of hydrodynamic dispersion in permeable rocks is of significant current interest in petroleum engineering. Understanding the transport properties of different fluids in oil bearing rock is critical to improving the efficiency of oil recovery. Nuclear Magnetic Resonance (NMR) has been applied in the laboratory to the measurement of flow propagators [1] in permeable rock cores; see for example ref. [2]. This technique has also been successfully implemented on comparatively low-field magnets [3]. Propagator measurements allow the displacement of encoded spins in a fluid to be observed under conditions of diffusion and flow. The NMR flow propagator is a probability distribution $P(\zeta,\Delta)$ of displacement $\zeta$ of spins in a fluid flowing with a superficial mean velocity $v_p$, after a flow observation time Δ. Information on the nature of the flow [2] can be obtained if the moments of the NMR propagator are acquired over a range of observation times.

Flow propagators can be obtained using established techniques such as the 13-interval Alternating Pulsed Gradient Stimulated Echo (APGSTE) pulse sequence [4]. Each individual measurement only probes a single mean displacement $\langle\zeta\rangle_0$ and so obtaining propagators with a range of mean displacements is an extremely time consuming process. For example, the accurate measurement of eight such propagators may require in excess of 7 h. Generally in the case of flow measurements in rocks, the total experimental time is not of concern since the system being studied is under steady-state conditions. However should a dynamic system be under investigation, such as the displacement of oil by water [5], this total experimental duration becomes critical. For such studies the implementation of a faster measurement technique is essential.

The rapid DiffTrain pulse sequence [6] probes a range of observation times, and hence mean displacements, in a single measurement. This technique has been shown to provide the same results as repeating the conventional APGSTE sequence for a range of observation times for water flowing through a bead pack [7] and has also been demonstrated as a viable method for rapid emulsion drop-

* Corresponding author.
*E-mail address:* lfg1@cam.ac.uk (L.F. Gladden).

1090-7807/$ - see front matter 
doi:10.1016/j.jmr.2007.12.014

let sizing [8]. A self-consistent cumulant analysis [9] is applied to the flow propagators recorded in this work to obtain the first (mean), second (standard deviation), and third (~skewness) moments of the displacement probability distribution. This paper details the combination of these two techniques and the first application of DiffTrain, featuring several modifications to increase its speed and robustness (as outlined in [10]), to the measurement of flow propagators in rocks.

Sparse $q$-space sampling [11] (where $q$ is the magnitude of the magnetisation wave vector) can additionally be used to reduce the experimental time. At high flow rates and/or long observation times, the signal variation and phase shift will be observed close to $q = 0$. Therefore by sampling only a selection of points with low $q$ values, a much more rapid measurement can be achieved. The precise range of $q$-space is defined by the range of data that can be well fitted by the cumulant expansion of $q^n$ up to $n = 3$. This is determined during the analysis process [2]. Whilst these selected data are unable to reproduce accurately the full displacement probability distribution, the first three propagator moments can be quantitatively obtained by appropriate fitting of the phase and signal amplitudes. If a suitable choice of the $q$-space sampling range is implemented, these moments can be calculated from very few data points, offering a further significant reduction in experimental time.

In studying transport processes within rocks the ability to determine, rapidly, the moments of the propagator distribution is important since a fluid undergoing Stokes flow through a porous matrix will demonstrate a power-law relationship between the mean and the standard deviation of displacement. This relationship can provide a relative measure of the nature of advective dispersion [12] which increases with pore space heterogeneity [2], and so can provide a further method of characterising the pore structure over various length scales in samples such as rock cores.

## 2. Experimental

The rock studied in these experiments is Bentheimer sandstone, a German outcrop material. Although the sandstone has a significantly higher permeability than most reservoir rocks, it exhibits small magnetic susceptibility variations and hence has low internal magnetic field gradients; as such it is ideal for use in these NMR studies [3]. A 3% KCl brine solution was pumped through the rock to prevent osmotic swelling of the clay content. The sandstone core had a porosity of $\varphi = 0.22$ and was cylindrical with a mean diameter of 38 mm and a length of 70 mm. To prepare the core for analysis, it was first dried, sealed in Perspex to prevent fluid transport across the radial surface of the rock core, and then vacuum saturated with brine. Distributor plates were added at each end to provide even flow across the whole sample cross-section.

The mean displacement $\langle\zeta\rangle_0 = v_p\Delta$ was calculated for a given observation time using the equation

$$v_p = \frac{Q}{A\varphi}, \tag{1}$$

where $v_p$ is the pore velocity (the mean velocity of fluid flowing in the rock pore space), $Q$ is the imposed volumetric flow rate, $A$ is the sample cross-sectional area, and $\varphi$ is the porosity. In these experiments, the imposed volumetric flow direction is along the $z$-axis which is the direction of the static magnetic field. Flow rates of $Q = 1$, 2, 5, 9, and 16 ml min$^{-1}$ were provided by a dual-cylinder piston pump [Teledyne ISCO Inc., USA; model D-250]. This corresponded, according to Eq. (1), to a maximum pore velocity of 1100 μm s$^{-1}$. $P(\zeta,\Delta)$ is determined by incrementing the gradient strength and recording the echo amplitude and phase at each value of the magnetisation wave vector, $\mathbf{q}$. The intensity of the acquired signal is proportional to the ensemble average of the polarised spins, $S(q) = \langle e^{2\pi i q\zeta}\rangle$, where $q = |\mathbf{q}| = \gamma_r\delta g_z/2\pi$ ($\gamma_r$ is the gyro-magnetic ratio of $^1$H, $\delta$ is the gradient pulse duration, and $g_z$ is the gradient strength along the $z$-axis). Since the signal $S(q) = \int P(\zeta',\Delta)e^{2\pi i q\zeta'}d\zeta'$, the inverse Fourier Transform (FT) of the echo intensities provides the probability distribution $P(\zeta,\Delta)$.

The DiffTrain pulse sequence is shown in Fig. 1, and is related to the conventional APGSTE pulse sequence, also shown in Fig. 1 for the specific case of a single value of $\Delta$ and $\alpha \equiv 90°$ pulse. The sequence uses two bipolar gradient pulses each of duration $\delta$ and strength $g_z$ to encode and decode the spins before and after a time $T_{start}$. Each pair of bipolar gradient pulses consists of an equal intensity positive and negative section of duration $\delta/2$. These are placed around a 180° radio frequency (RF) pulse to create the same diffusion weighting as a unipolar gradient pulse of duration $\delta$. The application of the split gradient reduces the influence of susceptibility induced magnetic field distortions [4]. The spin ensemble is stored along the $z$-axis during the time $T_{start}$, so the stimulated echo intensity depends on the $T_1$ recovery rather than the typically shorter $T_2$ relaxation decay. The observation time is given by $\Delta = T_{start} + 2\tau$, where $\tau$ is the inter-pulse encoding time. The whole experiment is repeated and the gradient strength incremented between $\pm g_z^{max}$ to probe the full range of $q$-space and hence provide $P(\zeta,\Delta)$.

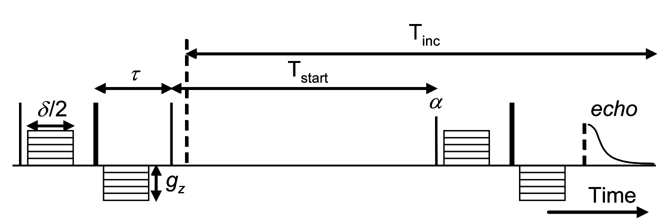


Fig. 1. The DiffTrain pulse sequence used for rapid diffusion and flow propagator measurements. The thin and thick vertical lines represent 90° and 180° pulses, respectively. The second half of a stimulated echo is recorded for each value of $\Delta_n$ in a single DiffTrain scan where $\Delta_n = (n-1) \times T_{inc} + T_{start} + 2\tau$. The gradients are ramped between $\pm g_z$ in subsequent scans. The APGSTE pulse sequence corresponds to the specific case of $n = 1$ and $\alpha \equiv 90°$.

The DiffTrain pulse sequence shown in Fig. 1 is an extension of the APGSTE sequence and uses the same phase cycle. Therefore any time saving that can be achieved in the APGSTE experiment through a reduction in the number of phase cycle steps can be applied equally to DiffTrain. Rather than acquiring a single echo, the decoding portion is repeated for multiple observation times. The observation times are then given by $\Delta_n = (n-1) \times T_{\text{inc}} + T_{\text{start}} + 2\tau$. By utilising an $\alpha$ pulse (where $\alpha < 90°$) only a fraction ($\sin\alpha$) of the polarised magnetisation is rotated onto the transverse plane for decoding in each interval. The tip angle of each $\alpha$ pulse was adjusted by varying the pulse power to satisfy the condition

$$e^{\frac{\Delta_1}{T_1}} \sin\alpha_1 = e^{\frac{\Delta_n}{T_1}} \sin\alpha_n \prod_{i=1}^{n-1} \cos\alpha_i, \tag{2}$$

thereby providing a constant unattenuated signal-to-noise (S/N) ratio for each echo [10]. The final $\alpha$ pulse can be set equal to a 90° pulse to acquire all the remaining magnetisation. The maximum number of observation times $n$ is limited by the $T_1$ recovery and the desired S/N ratio. The S/N ratio of each data point is obviously less by a factor of approximately $n$ than if acquired by the equivalent APGSTE measurement. In practice, however, the S/N ratio is rarely the limiting factor in these experiments.

The propagator measurements were conducted on a Bruker AV-85 spectrometer with a horizontal bore imaging magnet at 85 MHz ($^1$H) resonant frequency. In all cases the inter-pulse encoding time $\tau$ was set to 7 ms (the minimum possible time to incorporate the gradient pulses) to minimise signal loss from $T_2$ dephasing. All the gradient pulses were of duration $\delta = 4$ ms. The maximum gradient strength available was $g_z^{\max} = 10.7$ G cm$^{-1}$. For the dense $q$-space APGSTE and DiffTrain measurements, the gradients were ramped between $\pm g_z^{\max}$ in 128 equal steps. These data sets were converted into propagators and analysed using the method described by Scheven *et al.* [2] to obtain the propagator moments.

For the sparse $q$-space DiffTrain measurements, one set of data was acquired with 16 equal intervals to provide an approximate order of magnitude reduction in experimental time. The range of $g_z$ was then adjusted to appropriately sample $q$-space for each particular flow rate. For low flow rates ($Q = 1$ and 2 ml min$^{-1}$) the full gradient range, $\pm g_z^{\max}$, was utilised. For higher flow rates the specific gradient ranges used were $\pm 0.5 g_z^{\max}$, $\pm 0.25 g_z^{\max}$, and $\pm 0.1 g_z^{\max}$, to explore the corresponding flow rates of $Q = 5$, 9, and 16 ml min$^{-1}$ respectively. These ranges of $q$-space were chosen arbitrarily (within the constraint that gradient range decreased as $Q$ increased) in these experiments, although a more quantitative, optimised selection approach could be employed. This method allows for a more efficient sampling of $q$-space and hence can improve the robustness of the fit, especially at high flow rates and long observation times. The phase and amplitude of the signal were analysed to obtain the first, second, and third moments.

A typical dense $q$-space APGSTE sequence with 128 gradient increments, an 8 stage phase cycle, and $\Delta = 1$ s acquires a single flow propagator in 56 mins. Acquiring NMR flow propagators over 8 different observation times would therefore take approximately 7 h depending on the specific observation times. The equivalent dense $q$-space DiffTrain measurement takes only 67 mins and acquires $n = 8$ propagators with a series of increasing time increments, $T_{\text{inc}} = 5$–1000 ms, providing observation times ranging from $\Delta_1 = 16$ ms to $\Delta_8 = 2100$ ms. The sparse $q$-space DiffTrain acquisition as presented here takes only 9 mins, offering another significant decrease in the overall acquisition time. Additional DiffTrain data were recorded with the time increment fixed at $T_{\text{inc}} = 500$ ms at the highest imposed flow velocity ($Q = 16$ ml min$^{-1}$), thereby providing observation times up to $\Delta_8 = 4173$ ms. These latter DiffTrain measurements lasted slightly longer than the experiments described above (100 mins for the dense $q$-space sampling; 13 mins for the sparse $q$-space sampling). Although other fast NMR diffusion measurement techniques exist [13–15], DiffTrain offers the unambiguous capability to pre-determine the range of $\Delta_n$ and $g_z$.

Repeat dense and sparse $q$-space DiffTrain experiments with identical acquisition parameters and flow conditions revealed the measured mean displacement varied by less than $\pm 3\%$ even at the highest flow rates and longest displacements. This is comparable to the error associated with similar APGSTE measurements ($\pm 2\%$).

## 3. Data analysis

The first, second, and third moments of the propagator function: $\langle\zeta\rangle$, $\sigma^2$, and $\gamma^3$, are determined via a self-consistent cumulant analysis [9] by fitting the phase $\phi$ and absolute signal intensity $|S(q)|$, respectively, to

$$\phi(q) = \langle\zeta\rangle q - \frac{1}{6}\gamma^3 q^3 \tag{3}$$

and

$$\ln(|S(q)|) = -\frac{1}{2}\sigma^2 q^2. \tag{4}$$

The observed displacement $\langle\zeta\rangle$ will differ from the mean displacement $\langle\zeta\rangle_0$ by a factor $\theta = \langle\zeta\rangle / \langle\zeta\rangle_0$, where $\theta \geqslant 1$, due to enhanced surface relaxation. Any stagnant (trapped) spins are assumed to relax faster than those moving through the porous matrix. Therefore their contribution to the probability distribution at high displacements will be reduced and a shift in the mean is observed [16]. All the measured moments will be similarly affected. This can be compensated for by adding a Dirac delta function $\delta_{dd}(\zeta)$ such that the probability distribution becomes

$$P'(\zeta_0, \Delta) = (1 - \theta^{-1})\delta_{dd}(\zeta) + \theta^{-1} P(\zeta, \Delta), \tag{5}$$

where the prime (′) symbol denotes the corrected values. This artificially shifts the spectral weight of the distribution toward the stagnant population assumed to be undergoing zero displacement, compensates for the loss in signal, and hence re-establishes the expected mean displacement [16]. Accordingly, the corrected standard deviation ($\sigma'$) and skewness ($\gamma'$) can be deduced, respectively, from

$$\sigma'^2 = \frac{\sigma^2}{\theta} + \langle\zeta\rangle^2 \frac{\theta - 1}{\theta^2} \tag{6}$$

and

$$\gamma'^3 = \frac{\gamma^3}{\theta} + 3\langle\zeta\rangle\sigma^2 \frac{\theta - 1}{\theta^2} + \langle\zeta\rangle^3 \frac{(\theta - 1)(\theta - 2)}{\theta^3}. \tag{7}$$

The shape of the measured probability distributions can be characterised by the power law $\sigma'/\langle\zeta\rangle_0 \propto \langle\zeta\rangle_0^{\eta'}$, where $\eta'$ is the corrected power of the expected mean displacement. For measurements involving small displacements, molecular self-diffusion overwhelms the displacement due to flow [17] and the observed probability distribution is approximately Gaussian ($\eta' = -0.5$). Once the displacement due to the imposed flow exceeds the diffusion path length, the shape of the probability distribution will be related to the dispersion. In this pre-asymptotic regime $\eta' \geqslant -0.5$. Over comparatively long displacements, the probability distribution should return to a Gaussian (the asymptotic limit) and the ratio $\gamma'/\langle\zeta\rangle_0$ should tend to zero. However, in our implementation, the addition of the delta function means that this ideal limit will never be achieved. The uncorrected and corrected moments will form upper and lower limits on the true moments of the propagator. The uncorrected moments will be weighted by $T_1$ relaxation whilst the corrected moments restore the expected mean displacement but disproportionately weight the relaxation (and hence correction) to zero displacement; in reality relaxation will occur from across the displacement spectrum but preferentially for comparatively stagnant fluid, as must be the case since the measured value of $\theta$ is greater than 1.

## 4. Results and discussion

To determine the optimum pulse lengths to use in the DiffTrain measurement, the average spin-lattice relaxation times were recorded for the brine solution in the Bentheimer over the range of flow rates used in the propagator measurements. In all cases the average $T_1$ was observed to be $1.03\ \text{s} \pm 0.10\ \text{s}$, allowing appropriate pulse lengths to be determined for each value of $\Delta_n$ using Eq. (2). The tip angles of the pulses $\alpha_{i=1..n-1}$ varied from $p_t^\alpha = 12°–45°$. The final pulse ($\alpha_8$) had a tip angle $p_t^\alpha = 90°$. The pulse duration was kept constant at $t_p^\alpha = 15\ \mu\text{s}$ for all $\alpha$.

A selection of probability distributions obtained from a series of APGSTE measurements with dense (128 interval) $q$-spacing sampling can be seen in Fig. 2(a). These distributions have been scaled to the dimensionless function $P(\zeta) \times \langle\zeta\rangle_0$ plotted against the normalised displacement $\zeta/\langle\zeta\rangle_0$. In all cases the observed probability distributions are typical for flow through a Bentheimer sandstone sample [2,3]. At short observation times, the self-diffusion of the brine dominates and the probability distribution is

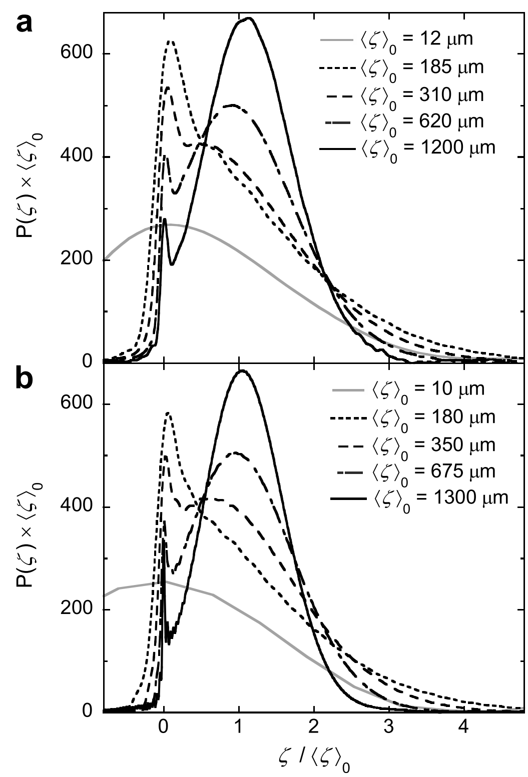


Fig. 2. A selection of probability distribution functions $P(\zeta,\Delta)$ for brine flowing through Bentheimer sandstone obtained from (a) multiple APGSTE experiments with observation times $\Delta = 20$, 300, 500, 1000, and 2000 ms, and (b) a single DiffTrain experiment with observation times $\Delta = 16$, 290, 563, 1095, and 2100 ms. In all cases the imposed flow velocity was $Q = 9\ \text{ml min}^{-1}$.

approximately Gaussian in shape (Fig. 2(a), grey line) [17]. At longer observation times, the mean displacement shifts to larger values, although a peak centred at $\zeta/\langle\zeta\rangle_0 = 0$ remains, signifying a stagnant volume of brine within the pores. As the mean displacement increases, the stagnant peak intensity is seen to decrease. The peak associated with the flowing spins increases in intensity accordingly. At long observation times (as $\Delta \to \infty$) and large displacements, the probability distribution is expected to return to a Gaussian as the asymptotic limit is approached. Practically however, the observation time is limited by the $T_1$ relaxation. In rock samples it is difficult to achieve a suitable combination of large displacements (high flow rate) and long observation times to completely explore this asymptotic regime. Almost identical displacement probability distributions can be seen in Fig. 2(b). These were acquired from a single dense $q$-space DiffTrain measurement under the same conditions as the data shown in Fig. 2(a). The slight discrepancies observed between Fig. 2(a) and (b) can be accounted for by the small variations in observation time at which the individual propagators were acquired.

The standard deviation of the probability distributions derived from dense $q$-space DiffTrain measurements are shown in Fig. 3. These data were obtained over a range observation times ($\Delta = 16–4173$ ms) and flow velocities

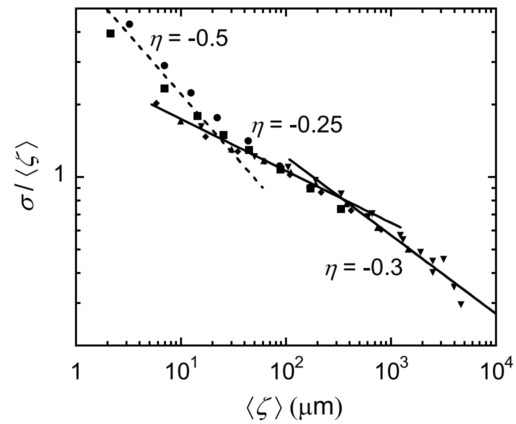


Fig. 3. Variation of the second moment of the flow propagators obtained using DiffTrain with linear $q$-spacing. The power law $\sigma/\langle\zeta\rangle \propto \langle\zeta\rangle^{\eta}$ fits give $\eta = -0.5$ (dashed line) in the diffusive regime at small displacements where the probability function is Gaussian in shape, and $\eta = -0.25$ in the first part of the pre-asymptotic regime where $20 < \langle\zeta\rangle < 300$ μm. For displacements where $\langle\zeta\rangle > 300$ μm, $\eta = -0.3$. The symbols reflect the imposed flow velocities: 1 (●), 2 (■), 5 (◆), 9 (▲), and 16 ml min$^{-1}$ (▼).

($Q = 1$–16 ml min$^{-1}$). At low displacements (within the diffusive regime) the power law fit to $\sigma/\langle\zeta\rangle \propto \langle\zeta\rangle^{\eta}$ yields $\eta = -0.5 \pm 0.03$ as expected for random molecular motions. There is a digression from this fit around $\langle\zeta\rangle = 20$ μm where dispersion becomes dominant over diffusion. The precise displacement at which this shift occurs will be dependent on the imposed flow rate. In the dispersion dominated region, $\eta = -0.25 \pm 0.02$. Over comparatively large displacements, $\langle\zeta\rangle > 300$ μm, the data are better fitted by $\eta = -0.3 \pm 0.05$; APGSTE data previously obtained from other Bentheimer rock cores yielded $\eta \approx -0.36$ [3] in this regime.

In order to account for any relaxation weighting from the measured propagator moments, $\sigma^2$ and $\gamma^3$ can be corrected according to Eqs. (6) and (7), respectively. Prior to this, the ratio of the measured to mean displacement $\theta = \langle\zeta\rangle/\langle\zeta\rangle_0$ needs to be determined. This ratio reaches a steady, velocity independent state at long observation times within the pre-asymptotic regime. A value of $\theta = 1.16$ was previously found for water flowing in Bentheimer rock samples measured at 85 MHz using the APGSTE sequence [3]. From the current dense $q$-space DiffTrain measurements a value of $\theta = 1.13$ was determined for a range of flow rates $Q = 1$, 2, 5, 9, and 16 ml min$^{-1}$; see Fig. 4 (solid circles). In the case of the sparse $q$-space DiffTrain data, Fig. 4 (open circles), a similar asymptotic increase to the same value of $\theta$ was observed.

The corrected standard deviation obtained from the dense and sparse $q$-space DiffTrain measurements can be seen in Fig. 5(a) and (b), respectively. These are shown for displacements above the diffusion dominated regime, $\langle\zeta\rangle > 20$ μm (determined from Fig. 3). The corrected standard deviation can be fitted by $\sigma'/\langle\zeta\rangle_0 \propto \langle\zeta\rangle_0^{\eta'}$ with $\eta' = -0.22$ in both cases. Good agreement is observed between these measurements and previous corrected AGPSTE data where $\eta' = -0.22$ for water flowing in sandstones [2]. It is important to note that all the corrected values of $\sigma'/\langle\zeta\rangle_0$ for $\langle\zeta\rangle_0 > 20$ μm are now well fitted by a single value of $\eta'$ regardless of flow rate.

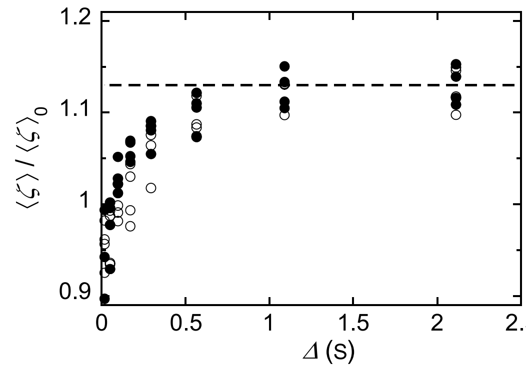


Fig. 4. Ratio of measured displacement $\langle\zeta\rangle$ to mean displacement $\langle\zeta\rangle_0$ for DiffTrain data with dense (solid circles) and sparse (open circles) $q$-spacing sampling. The horizontal dotted line indicates the asymptotic limit $\theta = 1.13$.

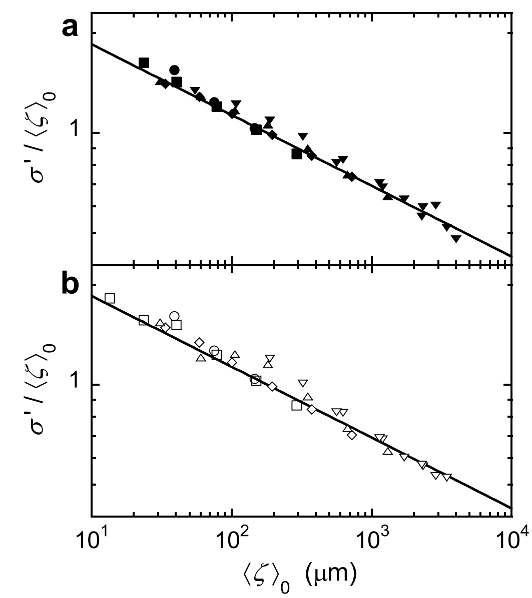


Fig. 5. Corrected, scaled standard deviation acquired using DiffTrain with (a) dense and (b) sparse $q$-space sampling. The power law fit to $\sigma'/\langle\zeta\rangle_0 = \langle\zeta\rangle_0^{\eta'}$ provided a value of $\eta' = -0.22$ (solid line) in both cases. The symbols reflect the imposed flow velocities: 1 (●), 2 (■), 5 (◆), 9 (▲), and 16 ml min$^{-1}$ (▼).

The corrected third moments should decrease asymptotically toward a value close to zero for increasing displacement as the probability distribution tends toward a Gaussian plus a delta function. As can be seen in Fig. 6(a) and (b) for the dense and sparse $q$-space DiffTrain data respectively, a smooth decay in $\gamma'/\langle\zeta\rangle_0$ is observed as expected.

All these data show the expected behaviour of the propagator moments as a function of displacement. The results from the dense and sparse $q$-space DiffTrain data are equivalent, despite the significant reduction in the amount of data acquired in the sparse sampling protocol. It should be noted that in all these DiffTrain measurements there is

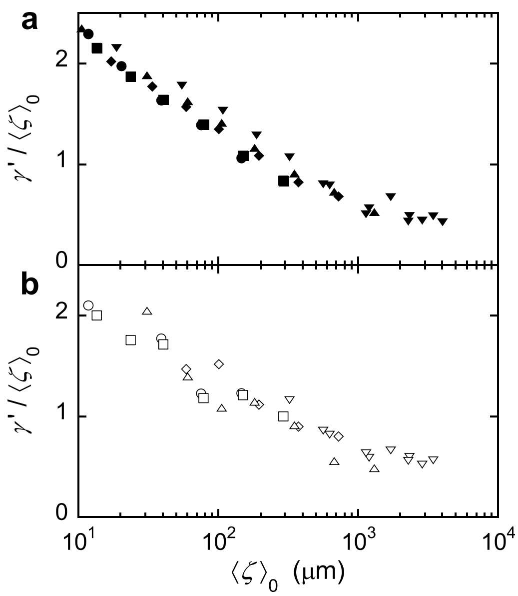


Fig. 6. Corrected, scaled skewness acquired using DiffTrain with (a) dense (b) sparse $q$-space sampling. The ratio $\gamma'/\langle\zeta\rangle_0$ decreases asymptotically toward a small, non-zero value as expected. The symbols reflect the imposed flow velocities: 1 (●), 2 (■), 5 (◆), 9 (▲), and 16 ml min$^{-1}$ (▼).

slightly more scatter on the mean displacement (Fig. 4) and skewness (Fig. 6) compared to the equivalent standard deviation data (Fig. 5). This is because the first and second moments are determined from the phase shift in the data, see Eq. (3), and are therefore more sensitive to the distribution of data points around $q = 0$. Due to the range of observation times inherent in a single DiffTrain measurement, it is difficult to find an optimum range of $q$-space sampling to suit all these observation times. In this work, an intermediate range was chosen for each experiment and it can be seen that this still provides an accurate measure for the moments of the propagator distribution.

## 5. Conclusion

The DiffTrain pulse sequence has been used to rapidly acquire NMR flow propagators for brine in Bentheimer sandstone over a range of observation times and flow rates. This reduced the experimental time required to determine the moments of 8 displacement probability distributions from 7 h (using the conventional APGSTE pulse sequence) to 67 mins. DiffTrain data was also acquired using sparse $q$-space sampling, further reducing the equivalent experiment time to only 9 mins. The flow propagators acquired using DiffTrain were nearly identical to those acquired using the conventional APGSTE technique. Furthermore, the behaviour of the propagator moments acquired using both dense and sparse $q$-space sampling with DiffTrain also corresponded to previous APGSTE studies on similar rock samples. The shift from diffusion dominated to dispersion dominated motion was clearly observed by analysing the second moment of the propagators. The corrected second and third moments displayed the expected dispersion behaviour for this high permeability sandstone. These techniques will allow accurate measurements of NMR flow propagator moments in time sensitive experiments such as displacement, dissolution, or deposition within reservoir rocks.

## Acknowledgments

We thank Dr. Uli Scheven, REQUIMTE/ CQFE, Portugal, for use of the propagator analysis protocol. J.M. thanks Dr. Belinda Akpa and Dr. Dan Holland for helpful discussions, and Dr. Silke Sheppard, Schlumberger Cambridge Research Ltd., for providing the samples. J.M. also thanks Schlumberger Cambridge Research Ltd. for financial support.

## References

[1] J. Karger, W. Heink, The propagator representation of molecular-transport in microporous crystallites, J. Magn. Reson. 51 (1983) 1–7.
[2] U.M. Scheven, D. Verganelakis, R. Harris, M.L. Johns, L.F. Gladden, Quantitative nuclear magnetic resonance measurements of preasymptotic dispersion in flow through porous media, Phys. Fluids 17 (2005) 117107.
[3] P.M. Singer, G. Leu, E.J. Fordham, P.N. Sen, Low magnetic fields for flow propagators in permeable rocks, J. Magn. Reson. 183 (2006) 167–177.
[4] R.M. Cotts, M.J.R. Hoch, T. Sun, J.T. Markert, Pulsed field gradient stimulated echo methods for improved NMR diffusion measurements in heterogeneous systems 83 (1989) 252–266.
[5] E.J. Fordham, M.A. Horsfield, C. Hall, L.D. Hall, Low-contrast secondary imbibition in long rock cores, Magn. Reson. Imaging 9 (1991) 803–808.
[6] J.P. Stamps, B. Ottink, J.M. Visser, J.P.M. van Duynhoven, R. Hulst, Difftrain: A novel approach to a true spectroscopic single-scan diffusion measurement, J. Magn. Reson. 151 (2001) 28–31.
[7] C. Buckley, K.G. Hollingsworth, A.J. Sederman, D.J. Holland, M.L. Johns, L.F. Gladden, Applications of fast diffusion measurement using Difftrain, J. Magn. Reson. 161 (2003) 112–117.
[8] K.G. Hollingsworth, A.J. Sederman, C. Buckley, L.F. Gladden, M.L. Johns, Fast emulsion droplet sizing using NMR self-diffusion measurements, J. Colloid Interface Sci. 274 (2004) 244–250.
[9] R. Kubo, M. Toda, N. Hashitsume, Statistical physics II: nonequilibrium statistical mechanics, Springer, Berlin, London, 1991.
[10] C.J. Davies, J.D. Griffith, A.J. Sederman, L.F. Gladden, M.L. Johns, Rapid surface-to-volume ratio and tortuosity measurement using Difftrain, J. Magn. Reson. 187 (2007) 170–175.
[11] P.P. Mitra, P.N. Sen, L.M. Schwartz, P. Ledoussal, Diffusion propagator as a probe of the structure of porous-media, Phys. Rev. Lett. 68 (1992) 3555–3558.
[12] P.G. de Gennes, Hydrodynamic dispersion in unsaturated porous-media, J. Fluid Mech. 136 (1983) 189–200.
[13] Y.Q. Song, X.P. Tang, A one-shot method for measurement of diffusion, J. Magn. Reson. 170 (2004) 136–148.
[14] Y.Q. Song, Multiple modulation multiple echoes: A one-shot method, Magn. Reson. Imaging 23 (2005) 301–303.
[15] Y.Q. Song, U.M. Scheven, An NMR technique for rapid measurement of flow, J. Magn. Reson. 172 (2005) 31–35.
[16] U.M. Scheven, J.G. Seland, D.G. Cory, NMR propagator measurements on flow through a random pack of porous glass beads and how they are affected by dispersion, relaxation, and internal field inhomogeneities, Phys. Rev. E 69 (2004) 021201.
[17] L. Lebon, J. Leblond, J.P. Hulin, Experimental measurement of dispersion processes at short times using a pulsed field gradient NMR technique, Phys. Fluids 9 (1997) 481–490.